

# *Crack Resistance and Toughening Mechanism of Nano-SiO<sub>2</sub> Reinforced PVA Fiber Cement-based Composites in Steel Bridge Engineering*

Edrise Zeinalli\*

Islamic Azad University, Iran

\*corresponding author

**Keywords:** PVA Fiber, Cement-Based Composite Material, Flexural Toughness, Crack Resistance and Toughness

**Abstract:** With the development of steel bridge engineering science, PVA fiber cement-based composite materials are gradually being explored and applied. Because of its high ductility and toughness, it has received extensive attention from academia and industry. Cement-based composite materials are essentially made of cement-related raw materials, which are mixed with various other materials to form composite materials. Incorporating Nano-SiO<sub>2</sub> into it can effectively improve the structural performance and durability of cement-based composite materials. Therefore, the purpose of this paper is to study the crack resistance and toughness mechanism of Nano-SiO<sub>2</sub> reinforced PVA fiber cement-based composites in steel bridge engineering. This paper first determined the design plan of the mix ratio of the Nano-SiO<sub>2</sub> PVA fiber cement-based composite material, and then used the composite beam composed of PVA fiber concrete and existing concrete as the experimental object. The test data shows that when the amount of hydrophilic nanopowder SiO<sub>2</sub> reaches 1%, the compressive strength of the mortar at the second and third day of age is increased. At this time, the higher the content of hydrophilic nanopowder SiO<sub>2</sub>, the higher its compressive and flexural strength. However, when the content is greater than 1.0%, the content of hydrophilic nano-powder SiO<sub>2</sub> has no great influence on the improvement of its compressive strength.

## 1. Introduction

In recent years, with the continuous development of modern building science, the requirements for the strength, hardness, toughness, crack resistance, durability and volume stability of concrete have become higher and higher [1-2]. Composite materials are widely used in the national steel beam engineering industry due to their excellent mechanical properties. Among them, the

development speed of fiber concrete is very fast, and it has become the fastest-growing new cement-based composite material in modern times. Among them, PVA fiber has attracted the most attention [3-4].

PVA fiber improves the internal structure of cement by increasing the contact area of the matrix concrete particles and the effective lap length of the fiber, and by forming a three-dimensional grid structure, it improves the internal structure of the cement and reduces the number and size of shrinkage cracks and small cracks in the matrix concrete. It prevents the unidirectional movement of the fiber, thereby forming a new stress area inside the fiber concrete, improving the integrity of the internal medium of the concrete, thereby enhancing the crack resistance and hardness of the cement base [5-6]. As a new material, nano- $\text{SiO}_2$  has shown broad application prospects in the field of steel bridge engineering because of its low manufacturing cost and strong toughening ability [7-8].

Regarding the research of PVA fiber cement-based composite materials, many scholars at home and abroad have conducted multi-angle discussions on it. For example, Wakeel S A selected two steel fibers of different sizes (different lengths and diameters) to be mixed into cement mortar. The total amount of fiber is 1.5%, which is used to study the influence of different mixing ratios of steel fibers on the mechanical properties of cement mortar materials. The research results show that: small-sized steel fibers can improve the strength of the material, while large-sized steel fibers can improve the material Toughness after peak strength. Steel fibers of different sizes can simultaneously increase the strength and toughness of the material under a specific mixing ratio, but they fail to show obvious strain hardening characteristics [9]. Selim A compared the pervaporation performance of single-mesh and double-mesh PVA fibers with operating temperature as a variable [10]; Laura studied the effect of PAA-coated magnetic nanoparticles on the performance of PVA-based hydrogels developed as environmental remediation devices [11]; Pouran studied the effect of zirconia disc delayed light curing cement on the microhardness and fracture toughness [12]; Xie T established a local interaction model of the bending behavior of PVA fiber concrete beams and GFRP steel bars [13]; J Yu conducted experiments on the fluidity and mechanical properties of steel-polyvinyl alcohol fiber concrete [14]; Khanikar T conducted research on the subject of PANI-PVA composite film-coated fiber probe as a stable and highly sensitive pH sensor [15]; Ahmad H conducted research on the application of nano MoWS<sub>2</sub>-rGO/PVA film as an all-fiber pulse amplitude modulator in the O band [16]; Luming studied the influence of collagen hydrolysate components on the preparation of collagen/PVA composite fibers [17]; Li X researched the crack resistance of cement stabilized crushed stone through experiments [18]; Zhao Y studied the polyvinyl alcohol fiber-reinforced cement-based composite material (PVA- ECC) Deterioration of behavior and microstructure changes after exposure to high temperatures [19]. It can be seen that the research on the characteristics of PVA fiber cement-based composites has gradually matured.

The innovations of this paper are: the basic principle and preparation test of the preparation of cement-based composite materials based on nano- $\text{SiO}_2$ , the design scheme of the mixing ratio of the test materials is determined; then the bending toughness test of the PVA fiber cement-based composite material is carried out to study the incorporation of PVA fiber and the influence on the bending toughness of cement-based composites; finally, the composite beam composed of PVA fiber concrete and existing concrete was used as the experimental object, and the relevant experiments were carried out under factors such as different concrete strengths and different PVA fiber concrete layer thicknesses, and rigorous exploration and analyzed the bending toughness of composite beams.

## 2. Mechanism of Crack Resistance and Toughness of Nano-SiO<sub>2</sub> Reinforced PVA Fiber Cement-Based Composites in Steel Bridge Engineering

### 2.1. PVA Fiber

The main physical properties of PVA (polyvinyl alcohol) are high modulus, high strength and low elongation; its chemical properties are acid and alkali resistance, corrosion resistance, and have good adhesion and compatibility with concrete, cement and other materials. Not only that, PVA fiber is also a non-toxic, non-polluting green building material.

According to related research studies, it is found that PVA organic polymer and cement-based materials can interact with each other to form a strong molecular combination, and they are evenly dispersed in the cement-based material to prevent cracking and strengthen the cement-based material. It is precisely because of this that PVA fibers have excellent bonding properties with cement-based materials.

### 2.2. PVA Fiber Cement-Based Composite Material Crack Resistance Performance

PVA fiber cement-based composite material has high tensile toughness and suitable tensile strength. The material based on PVA fiber cement can not only prevent the reduction of primary cracks on the upper part of the concrete, but also delay the appearance of harmful cracks on the surface. And the width of the cracking crack is kept within the range of less than 0.02mm during the loading process.

Under normal circumstances, cement-based materials will produce new cracks in other parts of the cross-section of the cement-based composite material when the fiber has not been pulled out or broken. Therefore, the stress and energy are dispersed on different cross-sections, which enhances the material's performance. Ductility, this is the multi-crack cracking stage of the material in the failure process [20]. However, PVA fiber cement-based composites have strong tensile strength. Once the cement base is cracked, there is a large bonding force between the fibers and the matrix, which can prevent the cracks from further extending outward. In the presence of microcracks, the blended fibers also act as aggregates, and cement hydration products will adhere to the surroundings, which reduces the generation of cement hydration and hardening microcracks to a certain extent, thereby improving the cement matrix Strength and toughness.

The plain cement-based composite material without fiber basically presents the form of brittle failure, and shows obvious strain softening characteristics after cracking. After the fiber is added, the cement and aggregate will bear the external load together when the test piece starts to undergo a change in force. When the load reaches a certain level, an initial crack will occur. The location of the crack is related to the size of the material defect. The crack at the beginning will be generated at the largest initial defect, the crack is affected by the size of the defect, and then new cracks are gradually generated from high to low, so that the crack will eventually form a crack [21].

However, the load-bearing capacity of the compatible materials with nano-SiO<sub>2</sub> and PVA fibers can be restored to the original load-bearing capacity immediately after an instant drop, even far exceeding the previous load-bearing capacity. If the crack is to continue to expand, it is necessary to overcome the bonding force or break or pull out the fiber in order to consume the breaking energy.

The stress is concentrated before the specimen of ordinary cement-based composite material without fiber is broken. After a main crack is formed on the surface of the specimen, the specimen will undergo brittle failure along the main crack with the continuous increase of the deformation.

When reaching the peak value, the specimen quickly cracked everywhere, and the axial load-deformation curve dropped rapidly [22]. The cement-based composite material mixed with PVA will absorb a lot of energy. Through the continuous increase of the deformation, the main cracks appear on the surface of the specimen, and a large number of micro cracks will also appear around the main crack. When the specimen reaches the maximum deformation, the specimen begins to undergo ductile failure, and the fibers in the gap between the main cracks begin to break, which consumes a lot of energy. Compared with the cracking failure of the non-fiber specimen, the specimen containing the fiber is completely destroyed at the end, and the specimen almost maintains its original shape. The bearing capacity of the material gradually decreases, and the axial pressure load-deformation curve also shows a slow downward trend. This shows that the ductility of the specimen with fiber is higher than that of the specimen without fiber, and the fiber can increase the cement-based composite material.

### 2.3. Mechanism of Nano-SiO<sub>2</sub> on the Crack Resistance of PVA Fiber-Reinforced Cement-Based Composites

The tensile strength of PVA fiber is much larger than that of cement stabilized crushed stone matrix. After being subjected to unidirectional tensile stress, the matrix will first produce micro-cracks. When the crack tip of the micro crack expands to an infinite distance from the fiber, the strong stress concentration near the crack tip will cause the fiber in the range to be partly separated from the matrix material along the bonding surface, thereby passing through the fiber [23]. Obviously, the range of this detachment before the fiber is not pulled out or broken is not too large. At the moment when the crack penetrates (or bypasses) the fiber, the sudden cracking of the cement stabilized crushed stone matrix causes a sudden change in strain on the separation interface between the fiber and the matrix, which in turn leads to a sudden change in stress, and the fiber that is penetrated by the crack is subjected to huge tensile stress[24]. When the crack has passed through a series of monofilament fibers but has not been pulled out or broken, as shown in Figure 1, the P series in the figure indicate the stress point, and the b series indicate the fiber tension. The sum of the reverse stress intensity factors produced by the superposition of these fibers is also very large, and the crack resistance effect is very obvious.

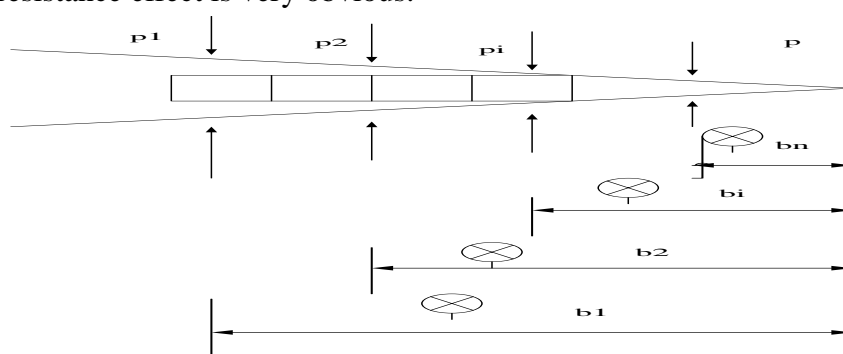


Figure 1. Cracks pass through a series of monofilament fibers

The above analysis fundamentally reveals the crack resistance process and crack resistance degree of PVA fiber, not only qualitatively expounds the crack resistance and toughening effect of PVA fiber on cement, but also quantitatively calculates the fiber crack resistance degree. Therefore, during the crack propagation process of the cement stabilized matrix, the PVA fiber produces a large amount of deformation and absorbs a large amount of deformation energy due to its high-strength

and high-modulus properties, and the effect of crack resistance and toughness is very significant.

Because nano- $\text{SiO}_2$  is a highly active admixture, it will generate  $\text{Ca(OH)}_2$  during the early chemical reaction with cement-based composite materials. Nano- $\text{SiO}_2$  can react with it quickly and reduce the concentration of  $\text{Ca(OH)}_2$  in the hydration process, will produce a greater heat of hydration [25]. Due to its small particle size, nano- $\text{SiO}_2$  has a strong filling effect. When early cracks occur, it can reduce the size and number of cracks, thereby enhancing the crack resistance of the material.

### 3. Experimental Method and Design

#### 3.1. Experimental Materials

(1) Cement. It adopts Huaxin brand cement with good workability.

(2) Flyash. The addition of fly ash can reduce the reaction between aggregates, improve the permeability of the matrix, and prevent the diffusion of chloride ions in the matrix. The selected fly ash has a particle size of 0.5 $\mu\text{m}$ ~2.0 $\mu\text{m}$  accounting for 80%, and the maximum particle size is 13.19 $\mu\text{m}$ , but the large particle size fly ash is very small.

(3) Water reducing agent. Water reducer is an additive commonly used in the mixing process of building materials. It can disperse cement particles well, maintain the slump of the slurry, improve the working performance of the good slurry, and enhance the performance of the unit mixture. It has a strong dispersing effect on cement particles, which can comprehensively improve or improve various properties of cement-based composite materials and reduce water consumption. The powder mass content of the water reducing agent in the experiment is 0.16~0.3% of the total weight of the gelling material, the color is white, the bulk density is 450-750  $\text{kg}/\text{m}^3$ , and the PH value is 9-11.4.

(4) PVA fiber. Compared with domestically produced PVA fibers, the use of K-II Colaron has a special surface treatment and has many advantages: low water absorption, good dispersion, etc. The specific values are: fiber density is 1.3  $\text{g}/\text{cm}^3$ , fineness is 15dtex, diameter is 0.04mm, shear length is 12mm, tensile strength is 1600MPa, elongation is 6%, and elastic modulus is 41GPa.

(5) Nano  $\text{SiO}_2$ : The indexes of Nano  $\text{SiO}_2$  used in the experiment are shown in Table 1.

Table 1. Nano  $\text{SiO}_2$  indicators data

Serial number	Test content	Test Results
1	Specific surface area	200 $\text{m}^2/\text{kg}$
2	content	99.6%
3	The average particle size	30nm
4	PH value	6
5	Performance density	55 g/l
6	Heating loss	1.0%(m/m)
7	Ignition loss	1.0%(m/m)

### 3.2. Test Mix Design

Table 2 shows the amount of each material in  $1 m^3$  nanoparticle  $SiO_2$  and PVA fiber-reinforced cement-based composite material.

Table 2.  $m^3$  Nanoparticle  $SiO_2$  and PVA Fiber Reinforced Cement-based Composite Material Consumption Table

Mixing ratio number	Water /kg	Cement/kg	Fly ash/kg	Fiber volume content (%)	Fiber content	Nano particles/kg	Sand/kg	Water reducing agent/kg
1	380	650	350	0.0	0	0	500	3
2	380	650	350	0.3	2.73	0	500	3
3	380	650	350	0.6	5.46	0	500	3
4	380	650	350	0.9	8.19	0	500	3
5	380	650	350	1.2	10.92	0	500	3
6	380	643.5	350	0.9	8.19	6.5	500	3
7	380	640.25	350	0.9	8.19	9.75	500	3
8	380	637	350	0.9	8.19	13	500	3
9	380	637	350	0.9	8.19	13	500	3
10	380	637.75	350	0.9	8.19	16.25	500	3

### 3.3. Production Process

The sample preparation process is as follows:

Step 1: Use an electronic scale with a measuring range of 2kg to weigh the various materials needed, mix part of the weighed water with the water reducing agent, and stir evenly with a glass rod; manually disperse the agglomerated PVA fibers to ensure the test process uniform dispersion of fibers.

Step 2: Using a planetary mortar mixer with a mixing drum capacity of 3L, first put the weighed fly ash, cement, and sand into the mixing pot and stir at low speed for 1 min, and then add the mixed water and water reducing agent and quickly stir for 2 min. And then add the PVA fiber at a uniform speed along the rotation direction of the mixing drum to ensure uniform dispersion. After stirring at high speed for 4-6 minutes, the specimen is formed.

Step 3: Put half of the slurry into the mold first, vibrate for 1 minute, put the remaining half of the slurry into the mold, continue to vibrate for 2 minutes, smooth the surface, and cover the surface of the sample with a plastic film.

Step 4: Disassemble the mold 24h after molding.

Step 5: After removing the mold, put it in a constant temperature and humidity curing room for 30 days at a temperature of  $20 \pm 2$  °C and a humidity of  $95 \pm 2$ %.

### 3.4. Device Improvement

An improved electro-hydraulic servo testing machine is used to conduct experiments on the displacement sensor. The improved displacement sensor can sensitively and accurately measure the

mid-span displacement distance, preventing the sensing part of the sensor from going deep into the bottom crack, causing displacement deviation to affect the overall data. At the same time, during the test, due to the limitation of the equipment supported by the support, the influence of the displacement of the support and the elastic deformation of the square steel frame, steel block, and foundation concrete were ignored.

### 3.5. Nano-SiO<sub>2</sub> Reinforced PVA Fiber Cement-Based Composite Material Crack Resistance Test

There are three methods to study the toughness of cement-based composites, as shown in Figure 2. In this experiment, the fracture toughness test was conducted.

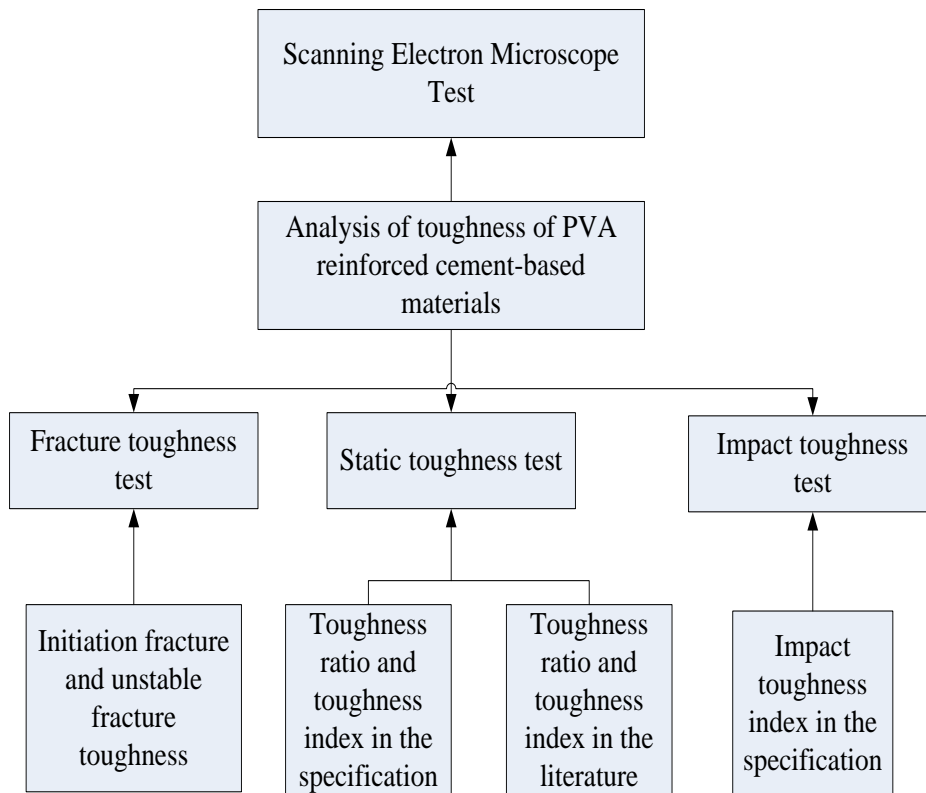


Figure 2. Research method of toughness of cement-based composites

#### (1) Compressive strength test

Toughness is an important reference for characterizing material mechanics. During the process of material deformation, the material will absorb part of the deformation energy, because different materials have different abilities to absorb deformation energy, so toughness is used to express the strength of the material's absorption capacity. Compared with brittle failure, the better the toughness of the material, the less likely it is that brittle failure will occur. Generally, a material with good toughness will undergo plastic failure with the increase of deformation, and its stress-strain curve shows nonlinear characteristics.

The entire area under the curve is the deformation energy of the material.

The PVA fiber cement-based composite material added with nano-A was tested for the compressive strength of a 70.7mm×70.7mm×70.7mm cube-shaped sample. Each group of samples was molded into 3 pieces, demolded after 24 hours and cured for 30 days respectively, and then tested for compressive strength. The equipment used in the test is a TYE-3000 pressure testing machine, the loading rate is 0.5 MPa/s, and the conversion factor is 1. Among them, C30 and C40 ordinary beams are set as the control group, and the specific test plan is shown in Table 3:

Table 3. Mix ratio of base concrete (unit: Kg/m<sup>3</sup>)

Specimen number	Base concrete strength	PVA fiber cement-based composite material layer thickness	Adhesive surface treatment form
C30	C30	-	-
C30-10- I	C30	10mm	smooth
C30-10- II	C30	10mm	Chisel
C30-20- I	C30	20mm	smooth
C30-20- II	C30	20mm	Chisel
C30-30- I	C30	30mm	smooth
C30-30- II	C30	30mm	Chisel
C30-40- I	C30	40mm	smooth
C30-40- II	C30	40mm	Chisel
C40	C40	-	-
C40-10- I	C40	10mm	smooth
C40-10- II	C40	10mm	Chisel
C40-20- I	C40	20mm	smooth
C40-20- II	C40	20mm	Chisel
C40-30- I	C40	30mm	smooth
C40-30- II	C40	30mm	Chisel
C40-40- I	C40	40mm	smooth
C40-40- II	C40	40mm	Chisel

Before the test, turn on the test machine and adjust the test machine to meet the requirements of this test. Then, place the test piece vertically on the bearing platform of the testing machine, and align it geometrically with the testing machine, while ensuring that the test piece is axially compressive during the test. The schematic diagram of the axial compression test is shown in Figure 3. During the test, the testing machine turns on the displacement control mode and the loading rate is set to 0.09mm/min. Perform the same operation on each test piece, record each operation data, and finally summarize and analyze the data.



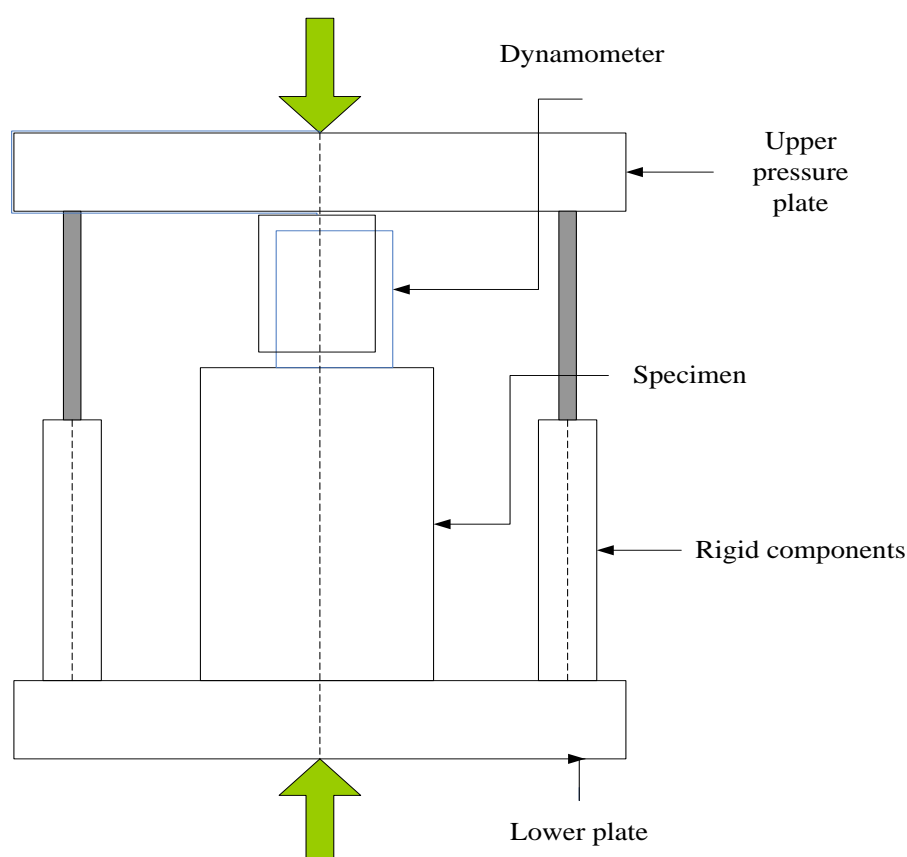


Figure 3. Axial compression test

### (2) Flexural strength test

The test materials are the same as before, and the preparation of the test piece is the second cold pouring. After 24 hours, remove and cure the pre-poured existing concrete (with a height of 60~90mm). After the test block is formed, cover the surface with plastic wrap, and pour the remaining thickness until the layer height is 100mm after 30 days. The raw materials used in the test are cement, fine sand, crushed stone, water reducing agent, PVA fiber and so on. Each group of samples was molded into 3 pieces, demoulded after 24 hours and cured for 30 days respectively, and then tested for flexural strength. After taking out the test piece, wipe off the moisture and impurities on the surface with a clean cloth, and check its appearance to ensure the smooth surface of the test piece, to prevent the test material from interfering with the test, and special circumstances during the test cause the waste of the test material and data unstable phenomenon. After the preparation work is completed, the test can be carried out.

Similarly, before the test, turn on the power of the testing machine, check and debug the testing machine to meet the requirements of this test. After that, put the test pieces in the flexural fixture one by one, and ensure that the test pieces are in the center of the testing machine. After the test pieces are damaged, record the failure load on the testing machine, and finally summarize and analyze the data.

### (3) Bend test

The size of the specimen is 40mm×40mm×160mm prism. The age of each specimen is 1 day, 3 days, 7 days, 14 days and 28 days. Three specimens are bent at four points for each group ratio.

After the test piece is poured, it must be cured in the standard curing room according to the specified age, and taken out for the experiment after the specified time. The experiment process is the same as the flexural strength test experiment.

The purpose of this experiment is to obtain the influence of fibers on the flexural performance of cement-based composites. The experiment mainly used the initial cracking strength, initial cracking mid-span deflection, ultimate flexural tensile strength, ultimate mid-span deflection, energy absorption capacity and toughness coefficient to evaluate the influence of fibers on the bending performance of this material. The equipment required for the experiment is shown in Figure 4:

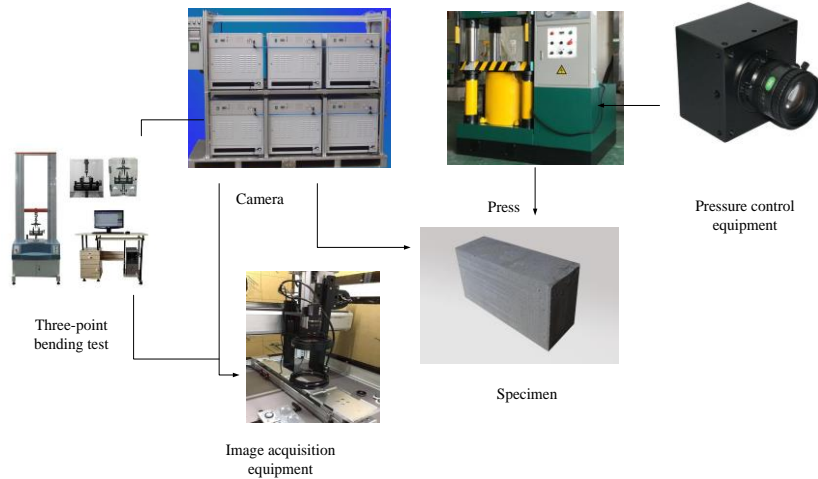


Figure 4. Three-point bending test

### 3.6. Test Indicators

#### (1) Anti-cracking performance

The sum of the cracking indexes of each crack is called the cracking index of the specimen, which is recorded as  $W$ , and the unit of cracking index is mm, which is calculated by formula (1):

$$W = \sum (A_i \cdot l_i) \quad (1)$$

In formula (1),  $W$  represents the cracking index in mm;  $A_i$  represents the weight value corresponding to a crack;  $l_i$  represents the length of the crack corresponding to the weight value. Among them, the crack width  $d \geq 3\text{mm}$ ,  $3 > d \geq 2\text{mm}$ ,  $2 > d \geq 1\text{mm}$ ,  $1 > d \geq 0.5\text{mm}$ ,  $d < 0.5\text{mm}$ , and the weight values  $A$  are 3, 2, 1, 0.5, 0.25, respectively.

The crack resistance ratio is the percentage of the difference between the average value of the crack index of the cement composite reference material and the average value of the crack index of the cement composite material to be tested divided by the average value. The calculation method of anti-cracking ratio  $\gamma$  is shown in formula (2), accurate to 1%.

$$\gamma = \frac{W_o - W_i}{W_o} \times 100 \quad (2)$$

In formula (2), the calculation result is greater than 0, indicating that the blended material can improve the anti-cracking performance of the cement-based composite material, and less than 0

indicates that the blended material reduces the anti-cracking performance of the cement-based composite material; the average value of the cracking index of cement-based composite materials mixed with fiber materials is represented by  $W_i$ , the unit is mm;  $W_o$  represents the average value of the cracking index of the cement-based composite material without other fiber materials, and the unit is mm.

(2) Flexural initial crack strength  $f_{cr}$

According to the initial crack load value, the flexural initial crack strength is calculated. The calculation method of flexural initial crack strength is shown in formula (3), and the calculation result is accurate to 0.1MPa.

$$f_{cr} = \frac{1.5F_{cr}L}{b^3} \quad (3)$$

In formula (3),  $f_{cr}$  represents the flexural initial crack strength (MPa) of the material;  $F_{cr}$  represents the initial crack load (N) of the material; L represents the distance between the test and the steel beam support (mm); b represents the test The side length of the material section (mm).

(3) Flexural toughness index

The calculation method of the bending toughness index of the material is shown in formulas (4), (5), (6), and the calculation result is accurate to 0.01.

$$I_5 = \frac{\Omega_{3\delta}}{\Omega_{\delta}} \quad (4)$$

$$I_{10} = \frac{\Omega_{5.5\delta}}{\Omega_{\delta}} \quad (5)$$

$$I_{20} = \frac{\Omega_{10.5\delta}}{\Omega_{\delta}} \quad (6)$$

In formulas (4), (5), and (6),  $\Omega_{\delta}$ ,  $\Omega_{3\delta}$ ,  $\Omega_{5.5\delta}$ , and  $\Omega_{10.5\delta}$  respectively represent the integral area under the load-deflection curve when the displacement is  $\delta$ ,  $3\delta$ ,  $5.5\delta$ , and  $10.5\delta$  (N.mm);  $I_5$ ,  $I_{10}$ ,  $I_{20}$  respectively represent the flexural toughness index of the load-deflection curve at different stages.

If the toughness of the tested cement-based material is close to the ideal elastoplastic material,  $I_5$ ,  $I_{10}$ , and  $I_{20}$  should not be less than 5, 10, and 20; if the tested cement-based material is an ideal brittle material, the values of these toughness indexes are all 1.

(4) Equivalent bending strength  $f_e$

The calculation method of the equivalent bending strength of the material is shown in formula (7). The calculation method is the same as the initial cracking strength by multiplying 1.5 on the basis of the original specification, and the calculation result is accurate to 0.1MPa.

$$f_e = \frac{1.5\Omega_k L}{b^3 \delta_k} \quad (7)$$

In formula (7),  $R_e$  represents the equivalent bending strength in MPa;  $\Omega_k$  represents the integral area under the load-deflection curve when the mid-span deflection is  $L/150$ , and the unit is  $N/mm$ ;  $\delta_k$  indicates the deflection value when the mid-span deflection is  $L/150$ , the unit is mm;  $b$  represents the side length of the section of the test piece, the unit is mm.

(5) Bending toughness ratio  $R_e$

The calculation method of material bending toughness ratio  $R_e$  is shown in formula (8):

$$R_e = \frac{f_e}{f_{cr}} \quad (8)$$

In formula (8),  $R_e$  represents the bending toughness ratio;  $f_e$  represents the equivalent bending strength (MPa);  $f_{cr}$  represents the flexural initial cracking strength (MPa).

## 4. Results and Analysis of Nano-SiO<sub>2</sub> on the Crack Resistance and Toughness of Reinforced PVA Fiber Cement-Based Composites

### 4.1. Influence of the Content of Different Hydrophilic Nano-SiO<sub>2</sub> on the Crack Resistance and Toughness of Cement

Adding hydrophilic nanopowder  $SiO_2$  to the cement slurry can reduce the void ratio of the mixed system, replace part of the filling water, increase the specific surface area of the system, and increase the amount of water absorbed. The influence of the content of different hydrophilic nano- $SiO_2$  on the crack resistance and toughness of cement is shown in Figure 5.

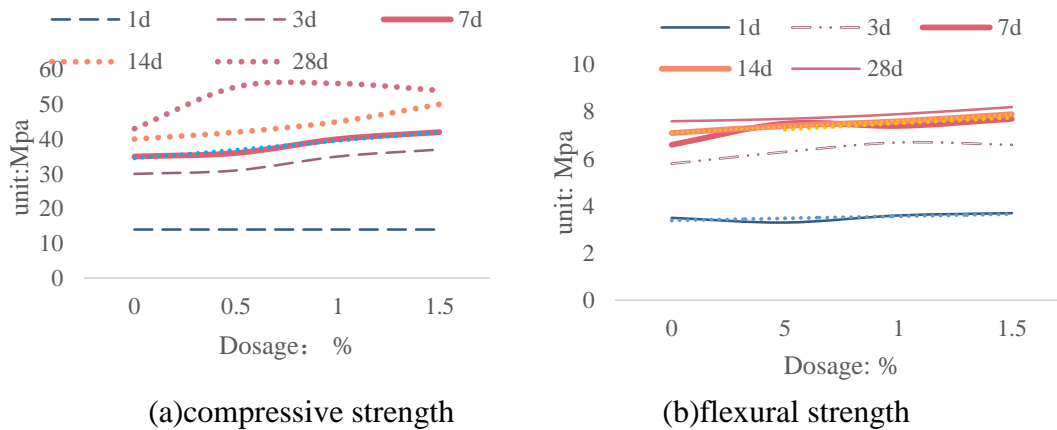


Figure 5. The influence of the content of different hydrophilic nano- $SiO_2$  on the crack resistance and toughness of cement

It can be seen from Figure 5 that when the mortar age is 1d, the hydrophilic nanopowder  $SiO_2$  does not affect its compressive strength and flexural strength, but in the later time, the hydrophilic nanopowder  $SiO_2$  has an effect and improves their compressive strength index. At the same time,

when the amount of hydrophilic nano-powder  $\text{SiO}_2$  reaches 1%, the compressive strength of the mortar at the second and third day of age is increased. At this time, the higher the content of hydrophilic nanopowder  $\text{SiO}_2$ , the higher its compressive and flexural strength. However, when the content is greater than 1.0%, the content of the hydrophilic nano- $\text{SiO}_2$  powder has no great influence on the improvement of its compressive strength. This is because although nano- $\text{SiO}_2$  powders have high pozzolanic properties, they have not yet produced large properties in the initial stage of hydration. As the hydration continues, the pozzolanic properties of nano-powders will gradually appear and strengthen. Therefore, there are many micron-level pores in the cement mortar, and without adding fiber materials, even if the amount of  $\text{SiO}_2$  is increased, its effect is limited.

#### 4.2. Analysis of Bending Toughness

The experimental material is divided into 5 test piece groups: P0, P0.5, P1.0, P1.5, P2.0, and the fiber volume of each group is 0,0.5,1.0,1.5,2.0, respectively. Calculate the energy absorption value of each group of specimens at each deflection, and the results are shown in Figure 6.

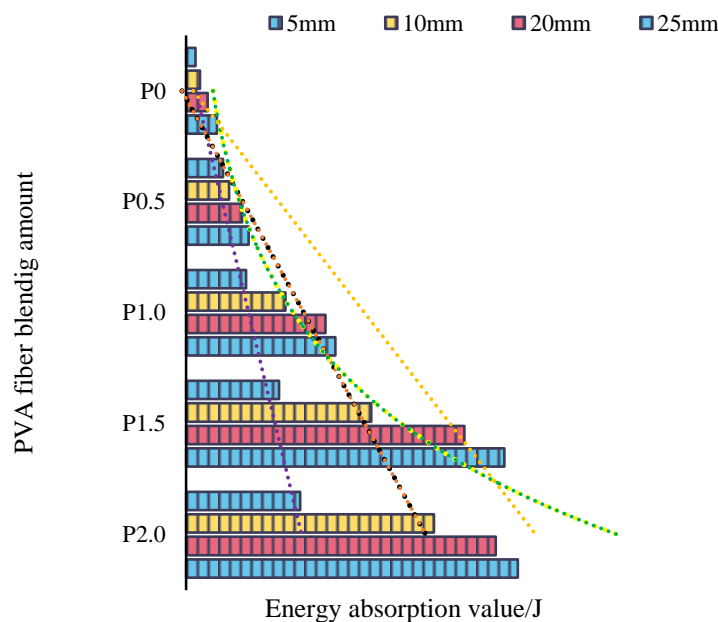


Figure 6. Energy absorption value of the specimen

Observing the Figure 6, it can be found that the energy absorption value of the P1.0 group is greater than that of the P0.5 group. This is because compared to P0.5, the number of fibers per unit volume in the P1.0 group is much greater than that in the P0.5 group, which has a stronger effect of preventing the continuous expansion and transmission of cracks, resulting in a large amount of energy being absorbed during the fiber pull-out process.

### 4.3. Test Board Toughness Index

The main results obtained by calculating the toughness index of the specimen are shown in Figure 7:

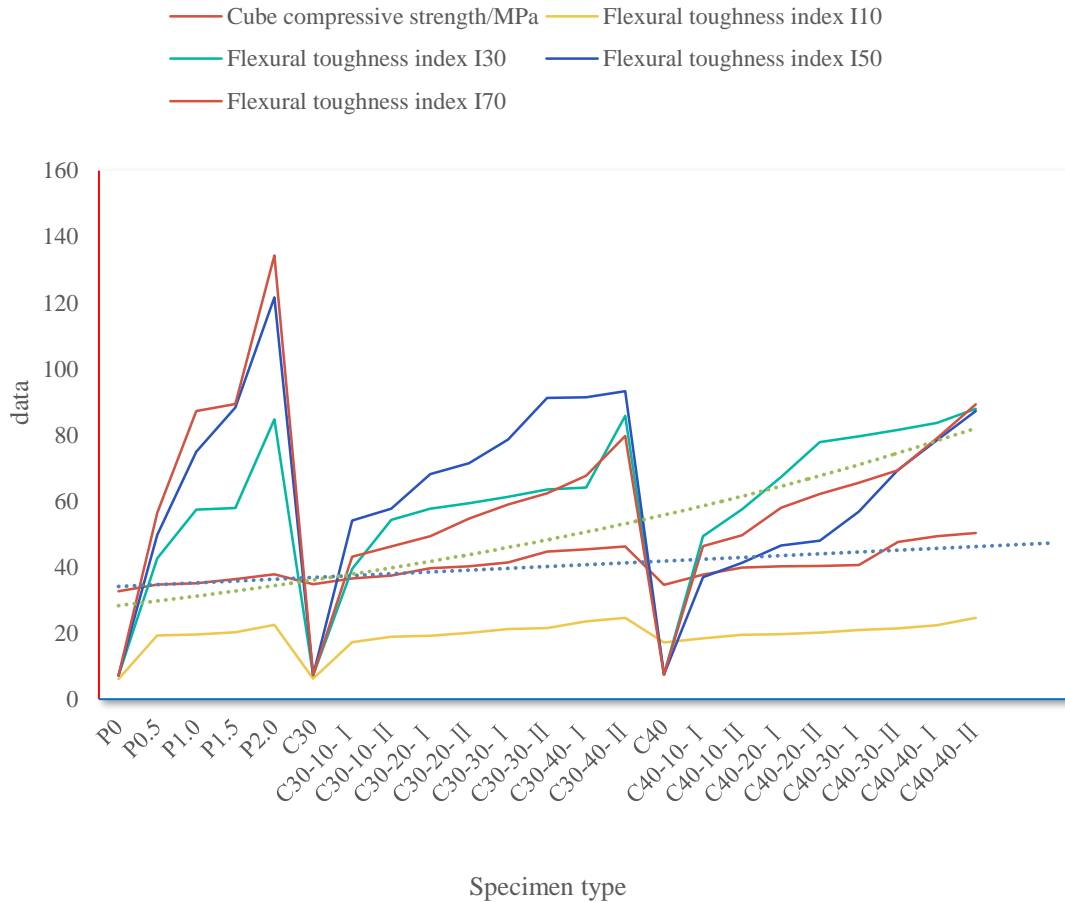


Figure 7. Main results of toughness index of test plate

(Note: P represents PVA fiber, and the number behind it represents the volume of PVA fiber.)

It can be found from Figure 7 that the flexural toughness index of the P0.5, P1.0, P1.5, and P2.0 groups are all expanding, and will increase significantly with the increase of the volume of PVA fiber. The flexural toughness indexes of the P0 group were 6.08, 7.14, 7.14, 7.14, while the volume of PVA fiber was 2.0%, and the P2.0 group was 37.79, 22.17, 84.76, 121.64, 134.36, which reached nearly 19 times that of the P0 group. It can be concluded that the volume of PVA fiber can improve the bending toughness of fiber cement-based composites, and the higher the content of PVA fiber, the toughness of the material can be greatly improved.

### 4.4. Test Data of Bending Load and Deflection

The results of the bending load deflection of each specimen are shown in Figure 8:

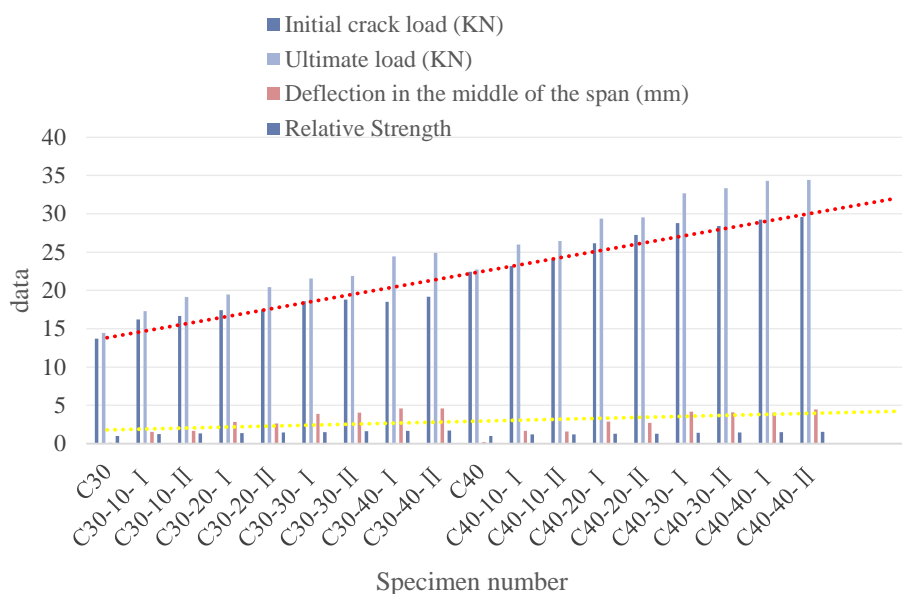


Figure 8. Results of bending load deflection of each specimen

It can be seen from Figure 8 that with the addition of  $\text{SiO}_2$  and PVA fiber materials, whether it is a composite beam with a matrix material of C30 or C40, the flexural bearing capacity of the composite beam specimen is significantly improved. It can be seen that the thickness of the cement-based material layer mixed with nano- $\text{SiO}_2$  and PVA fibers is increased, which significantly improves the ductility of the component.

## 5. Conclusion

The shrinkage and cracking of building materials of steel bridge engineering building materials can cause great damage to building materials. In order to alleviate such problems, this study is based on the basic principles and preparation tests of nano- $\text{SiO}_2$  cement-based composite materials, and the design scheme of the test materials is determined. Taking the composite beam composed of nano- $\text{SiO}_2$  mixed with PVA fiber concrete and existing concrete as the experimental object, relevant experiments were carried out under different factors such as the strength of concrete and the thickness of different PVA fiber concrete layers, and the bending toughness of the composite beam was carried out.

## Funding

This article is not supported by any foundation.

## Data Availability

Data sharing is not applicable to this article as no new data were created or analysed in this

study.

### Conflict of Interest

The author states that this article has no conflict of interest.

### References

- [1] Zhang Z , Zhang Q . *Matrix Tailoring of Engineered Cementitious Composites (ECC) with non-oil-coated, low tensile strength PVA fiber. Construction & Building Materials*, 2018, 161(FEB.10):420-431.
- [2] Shaikh F , Patel A . *Flexural behavior of hybrid PVA fiber and AR-Glass textile reinforced geopolymer composites. Fibers*, 2018, 6(1):2-2. <https://doi.org/10.3390/fib6010002>
- [3] Liu T Y , Zhang P , Wang J , et al. *Compressive Strength Prediction of PVA Fiber- Reinforced Cementitious Composites Containing Nano-SiO<sub>2</sub> Using BP Neural Network. Materials*, 2020, 13(3):521. <https://doi.org/10.3390/ma13030521>
- [4] Ito H , Watanabe K , Todoroki S , et al. *Study on Performance of PVA Fiber Reinforced Concrete Exposed for 10 Years to Seawater Spray. Journal of Advanced Concrete Technology*, 2018, 16(3):159-169. <https://doi.org/10.3151/jact.16.159>
- [5] Yoon H K , Kim S W , Jang Y I , et al. *Flexural Behavior Characteristics of Steel Tube Filled with PVA Fiber-reinforced Cement Composites (FRCCs) Incorporating Recycled Materials. Journal of the Korea Concrete Institute*, 2020, 32(3):275-283. <https://doi.org/10.4334/JKCI.2020.32.3.275>
- [6] Souza L D , Alavarse A C , Vinci M , et al. *The Synergistic Effect of Polymer Composition, Solvent Volatility, and Collector Distance on Pullulan and PVA Fiber Production by Rotary Jet Spinning. Fibers and Polymers*, 2021, 22(4):1-15. <https://doi.org/10.1007/s12221-021-0392-4>
- [7] Chen C , Li W , D Yang, et al. *Study on Autoclave Expansion Deformation of MgO-Admixed Cement-Based Materials. Emerging Materials Research*, 2017, 6(2):1-7. <https://doi.org/10.1680/jemmr.16.00090>
- [8] Wang Y , Zhi Q T , Zhao C , et al. *Reflection-Based Thin-Core Modal Interferometry Optical Fiber Functionalized With PAA-PBA/PVA for Glucose Detection Under Physiological pH. Journal of Lightwave Technology*, 2018, PP(99):1-1.
- [9] Wakeel S A , J Nēmeek, Li L , et al. *The effect of introducing nanoparticles on the fracture toughness of well cement paste. International Journal of Greenhouse Gas Control*, 2020, 84(2019):147-153. <https://doi.org/10.1016/j.ijggc.2019.03.009>
- [10] Selim A , Toth A J , Haaz E , et al. *Comparison of Single and Double-Network PVA Pervaporation Performance: Effect of Operating Temperature. Periodica Polytechnica Chemical Engineering*, 2020, 64(3):377–383. <https://doi.org/10.3311/PPch.15214>
- [11] Laura, M, Sanchez, et al. *Effect of PAA-coated magnetic nanoparticles on the performance of PVA-based hydrogels developed to be used as environmental remediation devices. Journal of Nanoparticle Research*, 2019, 21(3):1-16.
- [12] Pouran, Samimi, Sara, et al. *Effect of Delayed Light-Curing Through a Zirconia Disc on Microhardness and Fracture Toughness of Two Types of Dual-Cure Cement.. Journal of dentistry (Tehran, Iran)*, 2018, 15(6):339-350. <https://doi.org/10.18502/jdt.v15i6.326>
- [13] Xie T , Ali M , Visintin P , et al. *Partial Interaction Model of Flexural Behavior of PVA Fiber-Reinforced Concrete Beams with GFRP Bars. Journal of Composites for Construction*, 2018, 22(5):04018043.1-04018043.11.



- [14] J Yu, Zhai T , Liang X , et al. Fluidity and Mechanical Properties of Steel-PVA Fiber Reinforced Concrete. *Jianzhu Cailiao Xuebao/Journal of Building Materials*, 2018, 21(3):402-407.
- [15] Khanikar T , Singh V K . PANI-PVA composite film coated optical fiber probe as a stable and highly sensitive pH sensor. *Optical Materials*, 2019, 88(FEB.):244-251. <https://doi.org/10.1016/j.optmat.2018.11.044>
- [16] Ahmad H , Aidit S N , Tiu Z C , et al. Application of MoWS<sub>2</sub>-rGO/PVA thin film as all-fiber pulse and amplitude modulators in the O-band region. *Optical fiber technology*, 2019, 48(MAR.):1-6. <https://doi.org/10.1016/j.yofte.2018.12.011>
- [17] Luming, Yang, Jinwei, et al. Influence of collagen hydrolysate components on fabrication of collagen/PVA composite fiber:. *Textile Research Journal*, 2019, 90(9-10):1141-1148. <https://doi.org/10.1177/0040517519885020>
- [18] Li X , Lv X , Wang W , et al. Crack resistance of waste cooking oil modified cement stabilized macadam. *Journal of Cleaner Production*, 2020, 243(Jan.10):118525.1-118525.11.
- [19] Zhao Y , Yang X , Zhang Q , et al. Crack Resistance and Mechanical Properties of Polyvinyl Alcohol Fiber-Reinforced Cement-Stabilized Macadam Base. *Advances in Civil Engineering*, 2020, 2020(1):1-15. <https://doi.org/10.1155/2020/6564076>
- [20] Mouro C , Simes M , Gouveia I C . Emulsion Electrospun Fiber Mats of PCL/PVA/Chitosan and Eugenol for Wound Dressing Applications. *Advances in Polymer Technology*, 2019, 2019(1):1-11. <https://doi.org/10.1155/2019/9859506>
- [21] Hu Q , Li M , Li P , et al. Dual-wavelength passively mode-locked Yb-doped fiber laser based on a  $\text{SnSe}_2$ -PVA saturable absorber. *IEEE Photonics Journal*, 2019, PP(99):1-1.
- [22] Rui Z , Xu X , Bing C , et al. Fabrication of high-performance PVA/PAN composite pervaporation membranes crosslinked by PMDA for wastewater desalination. *Petroleum Science*, 2018, 15(01):1-11.
- [23] Kostagiannakopoulou C , Tsilimigkra X , Sotiriadis G , et al. Synergy effect of carbon nano-fillers on the fracture toughness of structural composites. *Composites Part B Engineering*, 2017, 129(nov.):18-25.
- [24] Zhang P , Li Q F , Wang J , et al. Effect of PVA fiber on durability of cementitious composite containing nano-SiO<sub>2</sub>. *Nanotechnology Reviews*, 2019, 8(1):116-127. <https://doi.org/10.1515/ntrev-2019-0011>
- [25] Ling Y , Zhang P , Wang J , et al. Bending resistance of PVA fiber reinforced cementitious composites containing nano-SiO<sub>2</sub>. *Nanotechnology Reviews*, 2019, 8(1):690-698. <https://doi.org/10.1515/ntrev-2019-0060>